The ISME Journal (2009) 3, 1301–1313
© 2009 International Society for Microbial Ecology All rights reserved 1751-7362/09 $32.00
www.nature.com/ismej

ORIGINAL ARTICLE

Mechanisms of transient nitric oxide and nitrous oxide production in a complex biofilm

Frank Schreiber, Birte Loeffler, Lubos Polerecky, Marcel MM Kuypers and Dirk de Beer
Max-Planck-Institute for Marine Microbiology, Bremen, Germany

Nitric oxide (NO) and nitrous oxide (N_2O) are formed during N-cycling in complex microbial communities in response to fluctuating molecular oxygen (O_2) and nitrite (NO_2^-) concentrations. Until now, the formation of NO and N_2O in microbial communities has been measured with low spatial and temporal resolution, which hampered elucidation of the turnover pathways and their regulation. In this study, we combined microsensor measurements with metabolic modeling to investigate the functional response of a complex biofilm with nitrifying and denitrifying activity to variations in O_2 and NO_2^-. In steady state, NO and N_2O formation was detected if ammonium (NH_4^+) was present under oxic conditions and if NO_2^- was present under anoxic conditions. Thus, NO and N_2O are produced by ammonia-oxidizing bacteria (AOB) under oxic conditions and by heterotrophic denitrifiers under anoxic conditions. NO and N_2O formation by AOB occurred at fully oxic conditions if NO_2^- concentrations were high. Modeling showed that steady-state NO concentrations are controlled by the affinity of NO-consuming processes to NO. Transient accumulation of NO and N_2O occurred upon O_2 removal from, or NO_2^- addition to, the medium only if NH_4^+ was present under oxic conditions or if NO_2^- was already present under anoxic conditions. This showed that AOB and heterotrophic denitrifiers need to be metabolically active to respond with instantaneous NO and N_2O production upon perturbations. Transiently accumulated NO and N_2O decreased rapidly after their formation, indicating a direct effect of NO on the metabolism. By fitting model results to measurements, the kinetic relationships in the model were extended with dynamic parameters to predict transient NO release from perturbed ecosystems.
The ISME Journal (2009) **3,** 1301–1313; doi:10.1038/ismej.2009.55; published online 11 June 2009
Subject Category: microbial ecosystem impacts
Keywords: microsensor; metabolic modeling; nitrification; denitrification; intermediates; nitrifier denitrification

Introduction

Nitric oxide (NO) and nitrous oxide (N_2O) are produced and consumed by catabolic reactions of bacteria involved in the biogeochemical N-cycle. These reactions are fostered by increased anthropogenic N input into the environment leading to a steadily increasing atmospheric N_2O concentration. This is of environmental concern, because the infrared radiative forcing potential of N_2O is $\sim$200 times that of CO_2, which makes N_2O a potent greenhouse gas (Stein and Yung, 2003). Moreover, NO and N_2O are involved in a set of catalytic reactions that transform ozone to molecular oxygen (O_2) in the stratosphere (Crutzen, 1979).

Correspondence: F Schreiber, Max-Planck-Institute for Marine Microbiology, Celsiusstr. 1, D-28359 Bremen, Germany.
E-mail: fschreib@mpi-bremen.de
Received 19 January 2009; revised 9 April 2009; accepted 16 April 2009; published online 11 June 2009

Denitrification and nitrification are generally considered to be the two main processes responsible for the formation of NO and N_2O (Stein and Yung, 2003). Heterotrophic denitrification is the respiratory, sequential reduction of nitrate (NO_3^-) or nitrite (NO_2^-) via NO and N_2O to N_2 (Zumft, 1997). The key enzymes in denitrification are nitrite reductase (Nir), nitric oxide reductase (Nor) and nitrous oxide reductase (Nos). NO levels in heterotrophic denitrifiers are well regulated, independent of NO_3^- and NO_2^- concentrations and are in the range of low nanomolar concentrations (Goretski *et al.*, 1990). NO consumption in heterotrophic denitrifiers might be mediated by widespread NO detoxifying enzymes, such as flavohemoglobins (Hmp or Fhp) and flavorubredoxin (NorVW), or respiratory NorB that can reduce NO to N_2O (Rodionov *et al.*, 2005).

Nitrification is the aerobic oxidation of ammonium (NH_4^+) performed by different groups of microorganisms. Aerobic NH_4^+ oxidation (Aox) to NO_2^- is performed by ammonia-oxidizing bacteria (AOB) or archaea (Arp and Stein, 2003; Konneke *et al.*, 2005).

In a next step, NO_2^- is oxidized aerobically to NO_3^- (Nox) by nitrite-oxidizing bacteria (NOB). Several studies have demonstrated the production of NO and N_2O by pure cultures of AOB (Kester *et al.*, 1997; Lipschultz *et al.*, 1981; Shaw *et al.*, 2006), but the mechanism is not completely understood. Generally two different pathways are inferred. First, the activity of hydroxylamine oxidoreductase (HAO) converts hydroxylamine (NH_2OH) to NO_2^- and releases small amounts of NO and N_2O (Hooper, 1968). Second, the activity of nitrifier-encoded Nir and Nor reduces NO_2^- to NO and N_2O in a process termed nitrifier denitrification (Poth and Focht, 1985; Bock *et al.*, 1995; Schmidt *et al.*, 2004). In both pathways, O_2 and NH_4^+ are required to form NH_2OH, the electron donor for NO_2^- reduction.

NO and N_2O turnover has also been studied in complex microbial communities. Studies in soils and nitrifying granules revealed that denitrification and nitrification are the contributing microbial pathways. Commonly, NO and N_2O accumulation increased with decreased O_2 and with increased NO_2^- and NH_4^+ concentrations (Conrad, 1996; Colliver and Stephenson, 2000; Kampschreur *et al.*, 2008).

Change in environmental conditions leads to transient production of NO and N_2O in pure cultures of AOB and heterotrophic denitrifiers (Kester *et al.*, 1997; Bergaust *et al.*, 2008), as well as in mixed microbial communities (Kampschreur *et al.*, 2008; Morley *et al.*, 2008). This transient production can lead to high concentrations and might thus contribute significantly to NO and N_2O emissions from various habitats. Despite the importance of transient NO and N_2O formation, the coupling and regulation of the responsible pathways remain poorly understood in complex microbial communities. This is primarily because the experiments on release of NO and N_2O from natural samples commonly rely on analysis of the headspace volume or the bulk solution, which have no spatial and low temporal resolution. However, local conversion rates and limited transport in aggregated or attached microbial communities lead to stratification and to microenvironments that are different from the bulk solution. Thus, high spatial resolution measurements of NO, N_2O and O_2 are required to distinguish between the contribution of aerobic (Aox) and anaerobic (heterotrophic denitrification) processes to NO and N_2O emission from stratified ecosystems where nitrification and denitrification co-occur. In addition, high temporal resolution measurements during system perturbation are a powerful method for unraveling complex sets of processes and to obtain insights into the coupling of different pathways.

The objective of this study was to assign NO and N_2O production to nitrifying or denitrifying processes occurring in a complex biofilm. Furthermore, we aimed to quantify the influence of O_2, of NO_2^- fluctuations and of metabolic state on the dynamics of the transient NO and N_2O formation. We conducted microsensor measurements with high spatial and temporal resolution to characterize *in situ* microenvironmental conditions, quantify the rates of the relevant processes and follow NO and N_2O formation upon perturbations. Furthermore, we developed a novel metabolic model that allowed numerical simulations of the measured NO transitions. On the basis of this model, we propose mechanisms that explain transient turnover of NO and N_2O by AOB and associated heterotrophic denitrifiers in the studied biofilm.

Materials and methods

Biofilm growth

Biofilms were grown in an aerated flow cell (~800 ml) using Tygon tubing as a surface for biofilm growth. The inoculum was obtained from a sewage treatment plant (Seehausen, Bremen) and was fed with medium at a flow rate of 1 ml min^{-1}. Biofilms with a thickness of 0.4–0.7 mm developed within 2–3 months in a medium consisting of 10 mM NH_4Cl and trace elements at final concentrations of 3 μM Na_2-EDTA, 1.5 μM $FeSO_4$, 77 nM H_3BO_4, 100 nM $MnCl_2$, 160 nM $CoCl_2$, 20 nM $NiCl_2$, 2.4 nM $CuCl_2$, 100 nM $ZnSO_4$ and 30 nM Na_2MoO_4 in tap water at pH 7.4. One month before the measurements, the medium was changed to a phosphate-buffered artificial freshwater medium containing 17 mM NaCl, 2 mM $MgCl_2$, 0.9 mM $CaCl_2$, 6.7 mM KCl and 1.5 mM KH_2PO_4/K_2HPO_4 (pH 7.5), supplemented with 400 μM NH_4Cl and trace elements as stated before. For microsensor measurements, small pieces of the biofilm-covered tubing were transferred into a smaller flow cell (~80 ml) placed in an aquarium. The aquarium served as a reservoir for 1.7 l of aerated artificial freshwater medium (with or without NH_4Cl) that recirculated through the small flow cell at a flow rate of 3 ml s^{-1} to create a constant flow of ~0.2 cm s^{-1} above the biofilm.

Experimental design

After biofilms adjusted to the conditions in the small flow cell for 1–2 days, steady-state microprofiles of O_2, pH, NH_4^+, NO_2^-, NO_3^-, N_2O and NO were measured in the presence of 400 or 0 μM NH_4Cl and at varying O_2 and NO_2^- concentrations in the overlying water. The metabolic response of the biofilms was studied by changing the conditions in the aquarium in the following sequence: (1) starting condition with O_2 at air saturation, (2) switching to low O_2 (~3% air saturation) by purging the medium with N_2, (3) addition of 3 mM $NaNO_2$ with O_2 at air saturation and (4) switching to low O_2 (~3% air saturation) in the presence of 3 mM $NaNO_2$. The response to the addition of 3 mM $NaNO_2$ at low O_2 was investigated in separate experiments. Transient concentration changes of NO, N_2O and O_2 were monitored inside the biofilm upon switching the

conditions until a new steady state was reached. The recirculated medium was sampled regularly to test for NO_3^- and NO_2^- accumulation from NH_4^+, stability of NH_4^+ concentrations, pH and temperature. NO_3^- and NO_2^- accumulated only in the presence of NH_4^+, and reached maximum concentrations of approximately 30 and 5 μM, respectively. NH_4^+ did not decrease below 370 μM. The temperature was 25–26 °C, and the pH was 7.2–7.3.

Microsensor measurements

Concentrations of O_2, N_2O and NO were measured with amperometric microsensors, whereas liquid-ion exchange microsensors were used for pH, NH_4^+, NO_2^- and NO_3^- measurements. Microsensors were prepared and calibrated as previously described (de Beer and van den Heuvel, 1988; Revsbech, 1989; de Beer *et al.*, 1997; Andersen *et al.*, 2001; Schreiber *et al.*, 2008). Vertical concentration profiles were measured with the microsensor mounted on a 3-axis micromanipulator (MM 33; Märzhäuser, Wetzlar, Germany). The vertical axis was motorized for μ-positioning (VT-80 linear stage; Micos, Germany, equipped with a 3564-K-024-BC motor, Faulhaber Group, Schönaich, Germany), and measurements were controlled by μ-Profiler software (www.microsen-wiki.net). The microsensor tip was adjusted manually to the sample surface with the help of a dissection microscope (Stemi SV 6; Carl Zeiss AG, Oberkochen, Germany).

Diffusive fluxes across the liquid–biofilm interface were calculated from the concentration gradients multiplied by the molecular diffusion coefficient D, as previously described. Values used for D were $2.34\times10^{-9}\,m^2\,s^{-1}$ for O_2, $1.98\times10^{-9}\,m^2\,s^{-1}$ for NH_4^+, $1.86\times10^{-9}\,m^2\,s^{-1}$ for NO_2^-, $1.92\times10^{-9}\,m^2\,s^{-1}$ for NO_3^-, $2.36\times10^{-9}\,m^2\,s^{-1}$ for N_2O and $2.21\times10^{-9}\,m^2\,s^{-1}$ for NO (Broecker and Peng, 1974; Li and Gregory, 1974; Zacharia and Deen, 2005).

Metabolic modeling of NO production

We developed an N-cycle model that couples processes involved in the production and consumption of NO, O_2 and NO_2^- in the biofilm (Figure 1). We assumed that NH_4^+ was aerobically converted to NO_2^- by Aox, and NO_2^- subsequently converted to NO_3^- by NO_2^- oxidation (Nox). Anaerobic conditions favor NO_2^- consumption by heterotrophic denitrification (hD). This results in the formation of NO, which is consumed in a sequential step by heterotrophic denitrification (hD-NO). Nitrifier denitrification by NH_4^+-dependent AOB (niD) produced NO aerobically from NO_2^-. Subsequently, NO is consumed by nitrifier denitrification (niD-NO). In addition, the model incorporated chemical NO oxidation with O_2 to NO_2^- (chem) and O_2 consumption by heterotrophic respiration (hR).

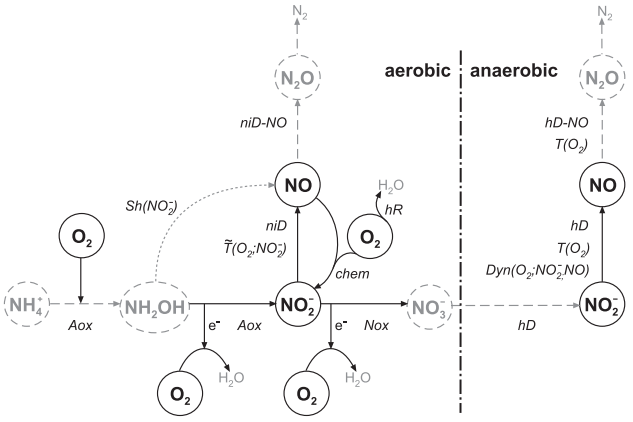

Figure 1 Schematic representation of the metabolic model of NO turnover in a complex biofilm. Pathways and compounds marked by solid black lines were calculated by the numerical model, whereas those marked with gray dashed lines were not calculated. Italic text next to the arrows indicates the pathways: Aox, ammonium oxidation; Nox, nitrite oxidation; niD, NO production by nitrifier denitrification; niD-NO, NO consumption by nitrifier denitrification; hD, NO production by heterotrophic denitrification; hD-NO, NO consumption by heterotrophic denitrification; hR, heterotrophic oxygen respiration; chem, chemical NO oxidation. Additional mechanisms that influence the rate of the respective pathway, with the compounds that affect those mechanisms in parentheses, are indicated by T, threshold; $\tilde{T}$, extended threshold; Dyn, dynamic function and Sh, shift function (see text and Equations (4)–(7) for details).

This model was implemented numerically in MATLAB (The MathWorks, Inc., Natick, MA, USA, the code is available at www.microsen-wiki.net) to describe the kinetic, metabolic and mass-transfer control of NO, O_2 and NO_2^- in the biofilm. We assumed that the biofilm was laterally homogeneous and transport was governed by diffusion. Thus, the dynamics of a solute with concentration C ($mol\,m^{-3}$) in and above the biofilm was described by a one-dimensional diffusion-reaction equation

$$\frac{\partial C}{\partial t} = D_C \frac{\partial^2 C}{\partial z^2} + R_C. \qquad (1)$$

Here, C denotes concentration of NO, NO_2^- or O_2, D_C is the corresponding diffusion coefficient in water ($m^2\,s^{-1}$), which was assumed to be constant throughout the biofilm and R_C ($mol\,m^{-3}\,s^{-1}$) is the net reaction rate at which the solute is produced or consumed. Both C and R_C were explicit functions of time t and depth z, with $z>0$ and $z<0$ corresponding to the biofilm and overlying water, respectively. The reactions for production and consumption of NO, O_2 and NO_2^-, as shown in Figure 1, were stochiometrically balanced and used to express the net reaction rates R_C for NO, O_2 and NO_2^- as

$$R_{NO} = 8R^{niD} - 4R^{niD-NO} + R^{hD} - 1R^{hD-NO} - 4R^{chem} \qquad (2a)$$

$$R_{O_2} = -1R^{niD} - 1R^{niD-NO} - 3R^{Aox} - 1R^{Nox} - 1R^{hR} - 1R^{chem} \quad (2b)$$

$$R_{NO_2^-} = -6R^{niD} + 2R^{Aox} - R^{hD} - 2R^{Nox} + 4R^{chem} \quad (2c)$$

Each individual rate was an explicit function of the concentrations of the solutes involved in the process and is described in detail in the Supplementary Table S1.

Kinetic control of the reaction rates R^i was described by the Michaelis–Menten law,

$$R^i(C) = v^i_{max} \cdot \frac{C}{K^i_C + C} = v^i_{max} \cdot M(C, K^i_C), \quad (3)$$

where K^i_C (mol m^{-3}) is the affinity constant of the process i to substrate C, v^i_{max} (mol m^{-3} s^{-1}) is the maximum rate of the process i and M denotes the Michaelis–Menten function describing the relationship between affinity and concentration without v_{max}. The affinity constants were obtained from the literature and the maximum rates were derived from the measured steady-state fluxes at the liquid–biofilm interface (as in Tables 1 and 2) divided by the biofilm thickness. The maximum rates of NO-consuming processes (niD-NO under oxic conditions and hD-NO under anoxic conditions) were determined by assuming that both processes were coupled to the respective production process. This allowed subtraction of the net NO production rate from the rate of the NO-producing process, which was determined from NO_2^- consumption.

Metabolic control of the reaction rates was implemented by combining information available from pure culture studies with postulated mechanisms based on data presented in this work. First, maximum activity of NO production (R^{hD}) and NO consumption ($R^{hD\text{-}NO}$) by heterotrophic denitrification occurred at micro-oxic to anoxic conditions, that is, at O_2 below a certain threshold concentration $\Theta^i_{O_2}$. This was implemented by multiplying the maximum reaction rates, v^{hD}_{max} and $v^{hD\text{-}NO}_{max}$, with a threshold function

$$T(C, \Theta^i_C, \delta^i_C) = \frac{1}{1 + \exp^{\frac{C-\Theta^i_C}{\delta^i_C}}}, \quad (4)$$

where δ^i_C represents the width of the concentration interval over which the threshold function changes from 1 to 0 (see Supplementary Figure S1). Furthermore, NO production by nitrifier denitrification (R^{niD}) was allowed only at low O_2 or high NO_2^- concentrations, which was achieved by multiplying the corresponding v^{niD}_{max} value with an extended threshold function (see Supplementary Figure S2)

$$\tilde{T}(NO_2^-, O_2, \Theta^{niD}_{NO_2^-}, \Theta^{niD}_{O_2}, \delta^{niD}_{NO_2^-}, \delta^{niD}_{O_2}) = \frac{1 - T(NO_2^-, \Theta^{niD}_{NO_2^-}, \delta^{niD}_{NO_2^-})}{T(O_2, \Theta^{niD}_{O_2}, \delta^{niD}_{O_2}) + T(NO_2^-, \Theta^{niD}_{NO_2^-}, \delta^{niD}_{NO_2^-})} \quad (5)$$

Threshold values were chosen by biological reasoning and by matching the concentration dynamics observed in the measurements.

Second, our experimental data suggested that after the O_2 concentration has decreased below a certain threshold, and when NO_2^- was simultaneously present in sufficient amounts, the rate of NO production by heterotrophic denitrification, R^{hD}, increased slowly with time (Figure 3d). This mechanism was implemented by further multiplying the v^{hD}_{max} value with the dynamic function

$$Dyn(t, t_0, \Delta t) = 1 - \exp^{\frac{-(t-t_0)}{\Delta t}}, \quad (6)$$

where t_0 is the time at which O_2 decreased below a threshold value $\Theta^{hD}_{O_2} - 2\delta^{hD}_{O_2}$ whereas NO_2^- was simultaneously present above 1 μM. The value of $\Delta t = 400$ s was estimated by fitting the measured

Table 1 Fluxes of measured solutes through the liquid–biofilm interface determined from microprofiles in a biofilm with the medium containing 400 μM NH_4Cl

Solute	*Flux (nmol cm^{-2} h^{-1})*[a]			
	5 μM NO_2^-[b]		*3 mM NO_2^-*[b]	
	100% O_2[c]	*<3% O_2*[c]	*100% O_2*[c]	*<3% O_2*[c]
NO	0.066 ± 0.024 (7)	1 ± 0.26 (10)	1.56 ± 0.49 (10)	0.92 ± 0.22 (7)
N_2O	2.53 ± 1.16 (7)	1.55 ± 0.36 (10)	4.72 ± 0.71 (7)	5.35 ± 2.68 (4)
O_2	−404 ± 44 (7)	−27 ± 9 (3)	−455 ± 56 (11)	−18 ± 8 (4)
NH_4^+	−168 ± 31 (6)	24 ± 11 (6)	−218 ± 28 (3)[d]	−48 ± 22 (3)[d]
NO_3^-	210 ± 30 (6)	21 ± 9 (3)	208 ± 37 (4)	−7 ± 2 (4)
NO_2^-	9.6 ± 3.6 (9)	−13.9 ± 5.5 (6)	−43 ± 15 (3)[d]	−67 ± 39 (3)[d]

[a]Fluxes are presented as mean ± standard error (number of profiles indicated in parentheses). Negative and positive values indicate net uptake and release of the solute, respectively.
[b]Nitrite concentration in the medium.
[c]Values are given as % air saturation in the medium.
[d]Measured at 250 μM NO_2^- instead of 3 mM NO_2^- because the sensitivity of the NO_2^- sensor was too low at 3 mM. However, 250 μM did not limit the uptake.

dynamic increase of NO in the presence of NO_2^- after the conditions in the overlying water were switched from oxic to suboxic (Figure 3d). In contrast, the dynamic increase of heterotrophic denitrification toward its maximum rate was accelerated to $\Delta t = 4$ s if NO was present above $\Theta_{NO}^{hD} = 0.32\,\mu M$. This assumption is based on reported evidence that NO serves as a signal for the expression of denitrification genes (Zumft, 2002, 2005).

Third, a shift mechanism (Sh) was implemented to model the instantaneous increase in NO concentration after NO_2^- was added under oxic conditions (Figure 4a). Reasoning for this mechanism was based on the assumption that HAO function is impaired by NO_2^-, leading to the release of NO that is reported to be an HAO-bound intermediate (Arp and Stein, 2003). This was implemented by removing a fraction f of the NO_2^- production rate by Aox from $R_{NO_2^-}$ in Equation (2c) and adding it to the total net NO production rate R_{NO} in Equation (2a) as a function

$$\mathrm{Sh}(t, t_0, \Delta t) = f \cdot R_{\mathrm{Aox}} . \exp^{\frac{-(t-t_0)}{\Delta t}} . \qquad (7)$$

Here, t_0 is the time when NO_2^- reached a threshold concentration of $\Theta_{NO_2^-}^{Sh} = 200\,\mu M$. The fraction of the shifted R^{Aox} decreased exponentially with time, resembling an adjustment of AOB metabolism after perturbation. The values of $f = 0.55$ and $\Delta t = 200$ s were estimated from the experimental data (Figure 4a).

The time-dependent diffusion-reaction equations (Equation (1)) were solved for all solutes using boundary conditions: (1) solute concentrations were fixed to the concentrations in the overlying water, C_w, at the top of the diffusive boundary layer (DBL), that is, $C(-z_{DBL}) = C_w$, and (2) the diffusive flux at the base of the biofilm was set to zero, that is, $\partial C/\partial z(z_B) = 0$, where z_{DBL} and z_B denote the thickness of the DBL and the biofilm, respectively. Experimental perturbations that resulted in O_2 decrease and NO_2^- increase in the medium were implemented by varying C_w over time. Experiments performed in the absence of NH_4^+ were modeled by excluding all processes from NO, NO_2^- and O_2 turnover that require NH_4^+ as electron donor, namely, Aox, nitrifier denitrification (niD) and NO consumption by nitrifier denitrification (niD-NO).

All parameters of the model are listed in Supplementary Table S1. When available, they were adjusted within a biologically reasonable range of values reported in the literature; otherwise, they were adjusted to match the experimental data presented in this work. In the paper, the model is used to interpret and discuss the experimental findings.

Results

Performance of the biofilm in steady state

For all compounds, the microprofiles showed either production or consumption within the entire biofilm. Stratified zones of production and consumption were not apparent (Figure 2 and Supplementary Figure S4). Thus, the overall performance of the biofilm was estimated from the fluxes across the liquid–biofilm interface (Table 1). Maximum potentials of Aox, Nox, nitrifier denitrification and heterotrophic denitrification were determined by creating the conditions such that only the process of interest occurred, and coupled processes were inhibited (Table 2).

The biofilm was fully oxic when the medium was aerated (Supplementary Figure S4A). In the presence of O_2, NH_4^+ was completely converted to NO_3^- with minor accumulation of NO_2^- (Supplementary Figure S4D), indicating that Aox and Nox occurred at similar rates (Tables 1 and 2). The coupling between Aox and Nox was not affected by addition of 3 mM NO_2^-. This was indicated by a similar 1:2:1 stoichiometry of NH_4^+, O_2 and NO_3^- fluxes in both

Table 2 Maximum activity of selected processes in the biofilm under different conditions

Process[a]	*Measured parameter*	*Condition* NH_4^+[b]/NO_2^-[b]/O_2[c]	J[d]	*Calculation*	*Rate of process*[e]
hR	O_2	0/0/100	−52	—	$J_{O_2}^{hR} = -52$
Nox	O_2	0/200/100	−154	$J_{O_2}^{Nox} = J_{O_2} - J_{O_2}^{hR} = 0.5 J_{NO_2^-}^{Nox}$	$J_{NO_2^-}^{Nox} = -204$
Aox	NH_4^+	400/5/100	−218	$J_{NH_4^+} = J_{NO_2^-}^{Aox}$	$J_{NO_2^-}^{Aox} = +218$
niD	NO_2^-	400/250/100	−43	$J_{NO_2^-}^{niD} = J_{NO_2^-} - J_{NO_2^-}^{Aox} - J_{NO_2^-}^{Nox}$	$J_{NO_2^-}^{niD} = -57$
hD	NO_2^-	0/250/3	−102	—	$J_{NO_2^-}^{hD} = -102$

[a]See Figure 1 for explanation of the abbreviations.
[b]Values are given in μM.
[c]Values are given as % air saturation.
[d]Flux (nmol cm^{-2} h^{-1}) through the liquid–biofilm interface presented as the net areal uptake rate of a certain solute by the biofilm.
[e]Gross areal rate (nmol cm^{-2} h^{-1}) of processes in the biofilm. Processes and compounds are indicated by superscript and subscript notations, respectively. Negative and positive values indicate consumption and production, respectively.

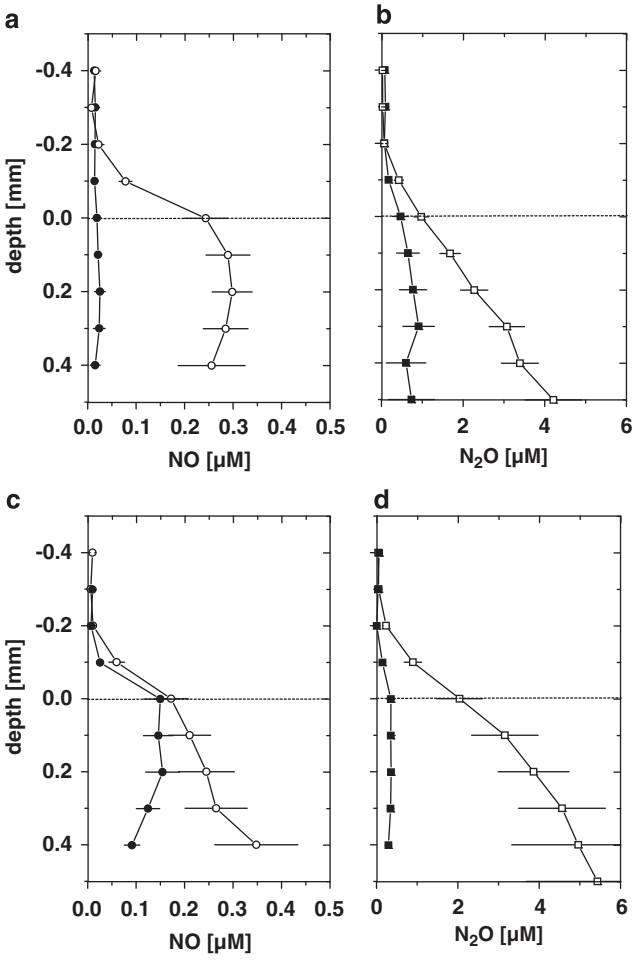

Figure 2 Averaged steady-state microprofiles of NO (**a** and **c**) and N_2O (**b** and **d**) in a complex biofilm. Microprofiles were measured in artificial freshwater medium containing 400 µM NH_4Cl with 5 µM NO_2^- (filled symbols) or with 3 mM NO_2^- (open symbols) and during aeration (**a** and **b**) or N_2 purging (**c** and **d**) of the medium. The dashed line represents the biofilm surface. Horizontal bars represent standard errors (number of profiles is given in Table 1).

the absence and the presence of NO_2^- (Table 1). However, nitrifier denitrification was induced by addition of NO_2^- in the presence of NH_4^+ and O_2. Nitrifier denitrification was indicated by the fact that the gross NO_2^- uptake, calculated from net NO_2^- uptake from the medium and NO_2^- production by Aox, exceeded the maximum NO_2^- consumption potential of Nox (Table 2). The remaining NO_2^- was reduced by AOB, with a rate that was ~20% of the NO_2^- production rate of Aox. Consumption of NH_4^+ and O_2 was slightly elevated in the presence of NO_2^- (Table 1).

In the absence of NH_4^+, the potential for heterotrophic processes was detectable, which were probably performed at the expense of reduced organic carbon present in the biofilm. Under oxic conditions, heterotrophic respiration of O_2 accounted for ~15% of the total O_2 consumption. In the absence of O_2, NO_2^- consumption by heterotrophic denitrification was ~50% of the NO_2^- consumption by NOB (Tables 1 and 2).

The effects of NO_2^- and O_2 on the formation of NO and N_2O in NH_4^+-containing medium are summarized in Table 1 and Figure 2. In the presence of NH_4^+ and high NO_2^-, NO and N_2O were produced regardless of the O_2 concentration in the medium. In contrast, at low NO_2^-, NO production was observed only under anoxic conditions, whereas N_2O production was low regardless of O_2. N_2O concentrations in the biofilm were an order of magnitude higher than NO concentrations, with NO ranging from <0.02 to 0.35 µM and N_2O from 0.35 to 5.4 µM. In the presence of high NO_2^-, the yields were 0.007 mol NO per mol NH_4^+ and 0.022 mol N_2O per mol NH_4^+. At low NO_2^-, the N_2O yield was reduced to 0.015 mol N_2O per mol NH_4^+ (Table 1). In the absence of NH_4^+ and NO_2^-, NO and N_2O fluxes were negligible regardless of O_2. However, in the absence of NH_4^+ and presence of NO_2^-, NO and N_2O were produced, but only under anoxic conditions (Supplementary Figure S6). The resulting fluxes were in the same range as those observed in the presence of NH_4^+ and NO_2^- under anoxic conditions.

Transient NO and N_2O formation in response to O_2 and NO_2^- changes

Upon the start of N_2 purging, O_2 decreased gradually in the biofilm until anoxic conditions were reached. The transient phase lasted ~7 min in the presence of NH_4^+ and ~12 min in the absence of NH_4^+ (Supplementary Figure S3). During this transition, highly dynamic concentration changes of NO and N_2O were detected with microsensors positioned in the biofilm at 200 µm depth (Figures 3a–d).

Decreasing O_2 concentrations in the presence of NH_4^+ caused a transient accumulation of NO and N_2O, which decreased to a new steady state after anoxic conditions were reached (Figures 3a and b). Although the accumulation was more pronounced at high NO_2^- concentration, the final steady-state levels were on average comparable to those observed at low NO_2^- (see also Figure 2c). Control measurements showed that in the absence of NH_4^+ and NO_2^-, NO and N_2O were neither produced nor consumed during the decrease of O_2 concentration (Figure 3c). In contrast, the absence of NH_4^+ at high NO_2^- concentration resulted in slow formation of NO and N_2O, starting shortly before anoxic conditions were reached (Figure 3d).

When NO_2^- was added under oxic conditions, NO concentration increased within less than a minute from below the detection limit to 1.2 µM, after which it decreased within 20 min to a new steady state. This was observed only if NH_4^+ was present (Figure 4a). In the absence of O_2, concentrations of NO increased upon the addition of NO_2^-. The presence of NH_4^+ did not influence the final NO steady-state concentrations, but affected the kinetics of its formation. NO formed slowly in the absence of

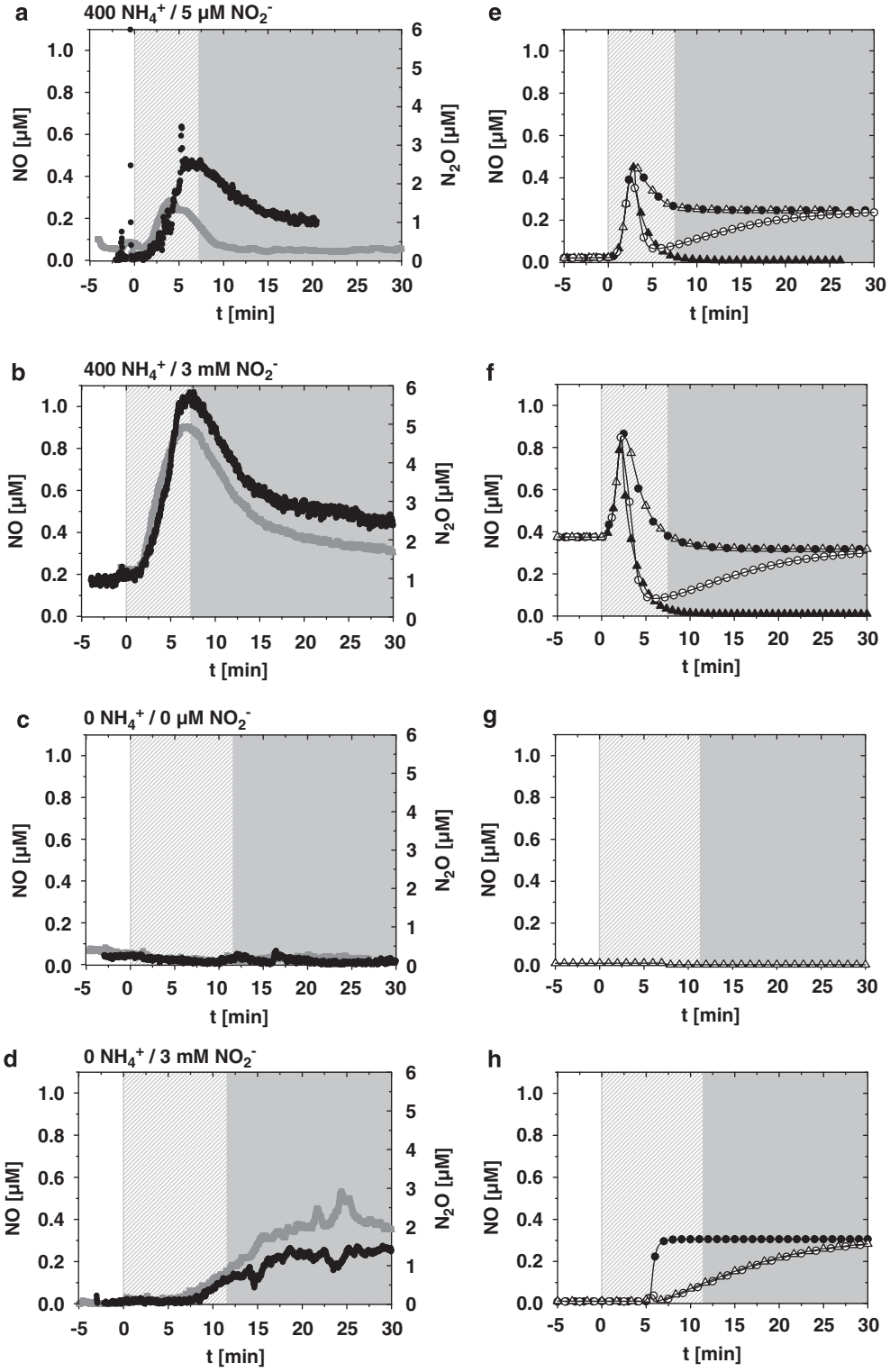

Figure 3 (**a–d**) Time series of measured NO (black line) and N_2O (gray line) concentrations with microsensors inserted in the biofilm at 200 µm depth. Purging of the medium with N_2 started at $t = 0$ min. (**e–h**) Time series of NO derived from the model shown in Figure 1. In each row, the boundary conditions and perturbations were implemented in the model such that they corresponded to the conditions applied during the measurement. Different stages of the model are shown, including (1) the model governed by kinetics and thresholds only (T and $\tilde{T}$; Equations (4) and (5); filled circles), (2) the model implementing the dynamic function (Dyn, Equation (6)) on heterotrophic denitrification (open circles), (3) the model implementing the dynamic function controlled by NO concentration (open triangles), (4) and the model implementing NO loss by diffusion after stopping all processes when the peak NO concentration was reached (filled triangles). White background indicates oxic, shaded areas indicate the transient phase from oxic to anoxic and gray areas indicate anoxic conditions. The medium composition with respect to NH_4^+ and NO_2^- is depicted at the top-left of each row.

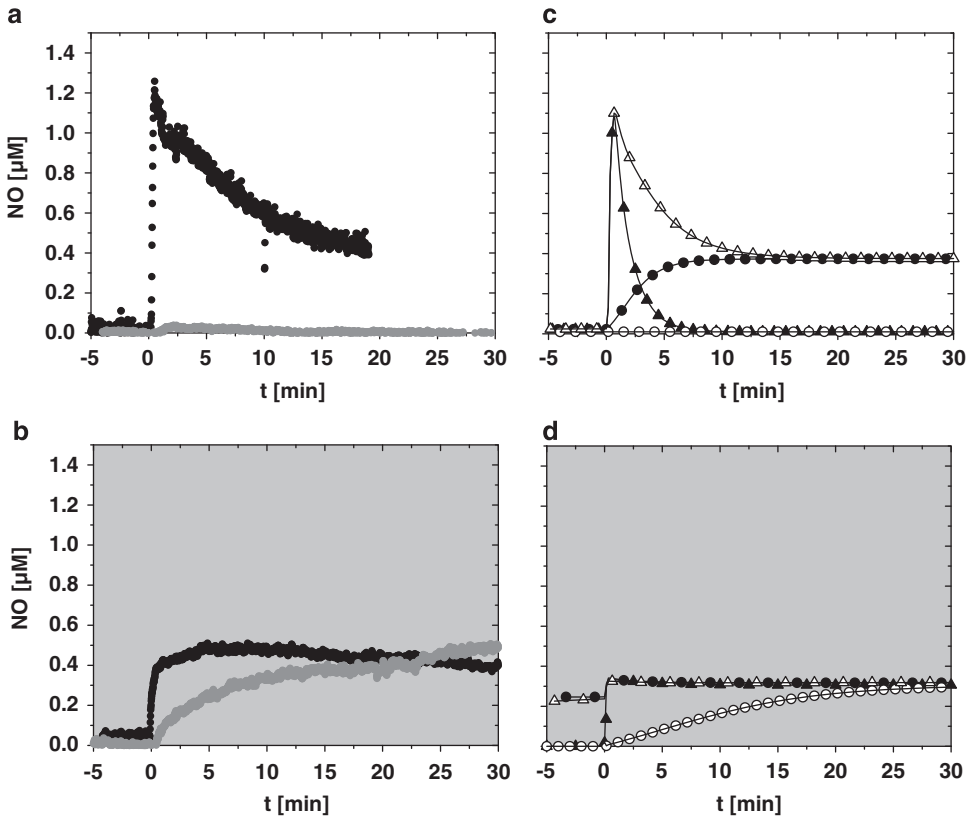

Figure 4 (**a** and **b**) Time series of NO measured with a microsensor inserted in the biofilm at 200 µm depth. 3 mM NO_2^- was added at $t = 0$ min to the medium containing 400 µM NH_4^+ and ~5/30 µM NO_2^-/NO_3^- (black line) or to the medium that did not contain NH_4^+ and NO_2^-/NO_3^- (gray line). White and gray backgrounds indicate oxic and anoxic conditions, respectively. (**c** and **d**) Time series of NO derived from the model (see Figure 1). In each row, the boundary conditions and perturbations were implemented in the model such that they corresponded to the conditions applied during the measurement. Different symbols depict different stages of the model. In panel (**c**), this includes the model governed by kinetics and thresholds only (filled circles), the model additionally implementing a shift function (Sh) that resulted in the production of NO instead of NO_2^- by Aox (open triangles), the model implementing NO loss by diffusion after stopping all processes when the peak NO concentration was reached (filled triangles) and the control condition where all NH_4^+-dependent processes were switched off (open circles). In panel (**d**), this includes the model governed by kinetics and thresholds only (filled circles), with the dynamic function added (open triangles) and the model in the absence of NH_4^+-dependent processes governed by kinetics and thresholds only (closed triangles) or with the dynamic function included (open circles).

NH_4^+. In contrast, the presence of NH_4^+, which resulted in low concentrations of NO_2^- and NO_3^- in the medium, caused an instantaneous increase of NO from slightly elevated levels (Figure 4b).

Discussion

Regulation of steady-state NO and N_2O production by ammonium oxidation under oxic conditions and by heterotrophic denitrification under anoxic conditions

NO and N_2O formation within a complex N-cycling community could be mediated by processes, such as Aox, Nox, heterotrophic denitrification or anaerobic oxidation of NH_4^+ (anammox) (Freitag *et al.*, 1987; Stein and Yung, 2003; Kartal *et al.*, 2007). Measuring the *in situ* activities and microenvironmental conditions enabled us to assign concomitant NO and N_2O formation to active processes.

Ammonium oxidation in steady state. AOB require NH_4^+ and O_2 to form NO and N_2O either by the HAO pathway or by nitrifier denitrification. The present data showed that NO and N_2O formation under oxic conditions depended on the presence of NH_4^+. NO and N_2O formation did not occur upon addition of NO_2^- when NH_4^+ was absent (Figure 4a, Supplementary Figures S6A and S6B). These experiments showed that under oxic conditions, NO and N_2O were formed by AOB, but not by NOB or (aerobic) heterotrophic denitrifiers. Previous studies emphasized the dependence of nitrifier denitrification on reduced O_2 and elevated NO_2^- concentrations (Lipschultz *et al.*, 1981; Poth and Focht, 1985; Kester *et al.*, 1997; Beaumont *et al.*, 2004a; Kampschreur *et al.*, 2008). Our experiments showed that nitrifier denitrification and simultaneous NO and N_2O formation occurs at high NO_2^- concentrations even if O_2 concentrations are high (Figures 2a and 4a and Supplementary Figure S4A). This was previously observed for *Nitrosomonas europaea* and *Nitrosospira* spp. (Shaw *et al.*, 2006). Moreover, it has been shown that denitrifying enzymes (NirK

and NorB) in *N. europaea* are expressed under fully oxic conditions (Beaumont *et al.*, 2004a, b).

In the model (Figure 1), NO production by nitrifier denitrification was kinetically controlled by O_2 and NO_2^-. The resulting steady-state NO concentration was kinetically controlled by the affinity of NO consumption by nitrifier denitrification to NO. However, NO production was only measured at high NO_2^- concentrations or under micro-oxic conditions. This indicates that NO accumulation under those conditions was controlled by NO production. To limit NO production in the model to high NO_2^- and low O_2 conditions, we implemented an extended threshold function ($\tilde{T}$, Equation (5), Supplementary Figure S2). This allowed an independent influence of O_2 and NO_2^- on NO production with a restricted maximum rate, excluding additive effects when both conditions were present at the same time.

Heterotrophic denitrification in steady state. Earlier studies have reported the ability of AOB pure cultures to produce NO under anoxic conditions (Kester *et al.*, 1997; Schmidt *et al.*, 2001) and reported that in a nitrifying mixed culture, NH_4^+ affected anaerobic NO formation in a concentration-dependent manner (Kampschreur *et al.*, 2008). Conversely, we found that under anoxic conditions, NO and N_2O formation did not depend on the presence of NH_4^+ and was only observed when NO_2^- and NO_3^- were present. This showed that heterotrophic denitrifiers, but not O_2-depending AOB, were responsible for NO and N_2O formation under anoxic conditions. The dependence of NO and N_2O formation on NO_2^- was confirmed under anoxic conditions in the absence of NH_4^+ (Supplementary Figures S6C and S6D). In the presence of NH_4^+, nitrification leads to accumulation of approximately 5 μM NO_2^- and 30 μM NO_3^- in the medium before N_2 purging. NO_3^- and NO_2^- served as electron acceptors for heterotrophic denitrification under subsequent anoxic conditions. This explains the formation of NO and N_2O under anoxic conditions by heterotrophic denitrification in the presence of NH_4^+ but not in its absence. Anammox could oxidize NH_4^+ and reduce NO_2^- under anoxic conditions, and could account for NO and N_2O formation. However, the biofilms grew under oxic conditions, which hamper growth of anammox bacteria (Strous *et al.*, 1997). Furthermore, NO_2^- uptake of the biofilm under anoxic conditions was similar in the presence and the absence of NH_4^+ (Tables 1 and 2), indicating that anammox did not contribute to additional NO_2^- reduction.

In the model (Figure 1), Michaelis–Menten kinetic dependence of heterotrophic denitrification on NO_2^- allowed NO production in the presence of NO_2^-, whereas threshold functions (T, Equation (4), Supplementary Figure S1) for O_2 restricted the process to anoxic conditions. The measured steady-state NO concentrations can be modeled (compare Figures 2a,c with Figures 3e,f and 4c,d) by kinetically controlling its accumulation with low K_m values for the NO consumption pathways, as has been described elsewhere (Betlach and Tiedje, 1981). As a result, steady-state NO concentrations under anoxia were more or less independent of NO_2^- concentrations, even though NO_2^- concentrations varied over ~3 orders of magnitude, corresponding to observations in pure culture studies (Goretski *et al.*, 1990). In addition, the K_m value of heterotrophic denitrifiers for NO_2^- was very low in the model, resulting in a minor increase of NO production due to the additional NO_2^-, because NO_2^- consumption was already saturated at low NO_2^- concentrations. In contrast, measured N_2O, the sequential product of NO reduction, showed a marked increase in the presence of high NO_2^- concentrations. Thus, in heterotrophic denitrifiers, accumulation of NO may not occur at high NO_2^- concentrations due to efficient reduction of NO to N_2O.

Furthermore, the model (Figure 1) showed that chemical NO consumption under oxic conditions was always several orders of magnitude lower than the biological rate, and contributed insignificantly to the total NO loss. Chemical production of NO from acidic decomposition of NO_2^- did not play a role, because the biofilm pH did not drop below 6.5 (Supplementary Figures S5A and S5B).

A recently described model was able to assign NO accumulation in a nitrifying reactor to nitrifier denitrification by implementing kinetic control and by modeling different production scenarios independent from each other (Kampschreur *et al.*, 2007). In our model, the use of threshold functions affected by O_2 and NO_2^- concentrations in addition to Michaelis–Menten kinetics enabled us to consider all possible NO-producing pathways simultaneously under varying conditions.

Perturbations of active ammonia oxidation and heterotrophic denitrification cause instantaneous NO and N_2O formation

The time series measurements showed that NO and N_2O reached transient maxima within the biofilm upon decreasing O_2 and adding NO_2^-. This phenomenon was also observed in studies with pure cultures of AOB and heterotrophic denitrifiers (Kester *et al.*, 1997; Bergaust *et al.*, 2008), as well as with mixed microbial communities (Kampschreur *et al.*, 2008; Morley *et al.*, 2008). However, these observations are not completely understood. We observed transient maxima of NO and N_2O only when either Aox or heterotrophic denitrification was actively performed before O_2 and NO_2^- changed. We conclude that the instantaneous formation of NO and N_2O is caused by perturbation of the active pathways on the enzyme level, resulting in an imbalance of the fine-tuned mechanisms that maintain NO homeostasis. NO and N_2O dynamics following perturbation were similar, demonstrating that they are sequentially produced by AOB and heterotrophic denitrifiers. The model can be

extended to N_2O concentrations if K_m values for N_2O reduction are available.

Heterotrophic denitrification in transient states. NO_2^- additions were followed by instantaneous NO formation, but only if NO_2^- and NO_3^- were present at low concentrations and if O_2 was absent before the perturbation (Figure 4b). Under such conditions, only heterotrophic denitrification can cause NO formation. The instantaneous formation of NO upon NO_2^- addition shows that NO-producing and NO-consuming enzymes are directly affected by NO_2^- and that *de novo* synthesis of enzymes cannot explain the dynamics. For example, it was demonstrated previously that NO_2^- can directly inhibit Nor (Kucera *et al.*, 1986; Kucera, 1992), which would lead to accumulation of NO. In addition, kinetics of NO_2^-- and NO-reducing enzymes might allow NO accumulation depending on the NO_2^- concentration. Instantaneous NO production was modeled by assuming that full expression of heterotrophic denitrification potential requires the absence of O_2 and the presence of NO_2^- (Zumft, 2005). Under conditions allowing full expression of heterotrophic denitrification, kinetics explained the instantaneous increase of NO upon addition of NO_2^- in the model (Figure 4b, black line and Figure 4d, filled circles).

In contrast, measured NO increased slowly if the conditions before the perturbation did not allow full expression of denitrification (that is, the presence of O_2 or absence of NO_2^-; Figure 3d, black line and Figure 4b, gray line). We assumed that in these cases, removal of O_2 (Figure 3d) or addition of NO_2^- (Figure 4b) results in the expression of denitrification enzymes. The subsequent slow NO increase was modeled by implementing a dynamic function (Dyn; Equation (6)) in addition to the kinetic control (Figures 3h and 4d open circles). Modeling without the dynamic function resulted in an instantaneous increase of NO for transients upon O_2 removal and NO_2^- addition (Figure 3h, filled circles and Figure 4d, filled triangles), because in this case the expression of heterotrophic denitrification was assumed to be constitutive. This shows that the requirements for the expression of enzymes for heterotrophic denitrification, and their slow expression when all conditions are met, need to be included when modeling transient NO accumulation.

Ammonium oxidation in transient states. The measurements showed that NO formed instantaneously if O_2 was removed or NO_2^- was added, but only if NH_4^+ was available to allow active Aox before the perturbation. AOB form NO and N_2O by the HAO pathway or by nitrifier denitrification (Arp and Stein, 2003). Both pathways might contribute to NO and N_2O formation, but cannot be separated from each other by our experiments. Our model showed that the instantaneous transient increase of NO caused by AOB upon NO_2^- addition (Figure 4a) cannot be explained solely with NO production by nitrifier denitrification. Here, NO increased slowly to steady state because of the delayed diffusion of NO_2^- into the biofilm matrix (Figure 4c, filled circles). The transients upon NO_2^- addition were satisfactorily modeled by implementing a shift function (Sh; Equation (7)), which resulted in the production of NO instead of NO_2^- from NH_4^+ when NO_2^- concentrations increased above a certain threshold ($\Theta^{Sh}_{NO_2^-} = 200\,\mu M$) (Figure 4c, open triangles). The successful use of this function supports our hypothesis that NO formation by AOB occurs if their active metabolism is disturbed by NO_2^- that possibly impairs the smooth functioning of HAO (Arp and Stein, 2003).

AOB-dependent transient increase of NO during O_2 decrease in the model resulted from a micro-oxic threshold imposed on NO production by nitrifier denitrification ($\Theta^{niD}_{O_2} = 40\,\mu M$) (Figures 3e and f, filled circles). The increase of NO during micro-oxic conditions was not counteracted by NO consumption due to nitrifier denitrification (niD-NO) because O_2 disappeared before the K_m value for NO (0.6 μM) was reached. Rather, the onset of anoxia resulted in the decline of NO production by nitrifier denitrification (niD) because of kinetic limitations by the substrate O_2. The modeled results suggest that nitrifier denitrification metabolism is fully expressed under oxic conditions as reported by Beaumont *et al.* (2004a), resulting in instantaneous NO formation upon reduced O_2 concentrations. This increase cannot be counteracted until NO accumulates to concentrations equal to the K_m value of the NO consumption pathway.

Direct regulation of NO and N_2O decrease after its transient accumulation

NO and N_2O decreased to a new steady-state level after they reached peak concentrations upon O_2 and NO_2^- concentrations were changed. NO concentrations were always one order of magnitude below N_2O, indicating that regulation of potentially cytotoxic NO (James, 1995) is more critical than that of nontoxic N_2O, and that the K_m value of N_2O reduction is higher than that of NO reduction. The decrease of NO within minutes after the accumulation of NO indicates that genetic regulation cannot explain the dynamics. Instead, different metabolic pathways governed NO turnover after the conditions changed, or enzymes were directly affected after the peak was reached, for example, by inhibition.

NO decrease after O_2 removal. The pathways governing NO turnover switched from nitrifier denitrification to heterotrophic denitrification between oxic and anoxic conditions (Figures 3a and b). Directly after nitrifier denitrification stops, heterotrophic denitrification cannot instantaneously start, as the enzymes must be expressed. Therefore, modeling with the dynamic function (Dyn; Equation (6)) showed a transient NO minimum when reaching anoxia,

because NO was lost from the biofilm by diffusion and increased slowly thereafter (Figures 3e and f, filled triangles and open circles). However, we did not measure such a minimum, indicating that NO production continued directly after the transition. Possible explanations are that either nitrifier denitrification continued or the dynamic of expression of heterotrophic denitrification (Dyn, Equation (6)) was enhanced in the transient phase in response to NO. Modeling showed that the later scenario was not biologically feasible, because the expression of heterotrophic denitrification needed to be enhanced to be 100-fold ($\Delta t = 4$ s instead of 400 s) faster than was calculated for the onset denitrification upon reduced O_2 (Figures 3e and f, open triangles and Figure 3h, open circles). Alternatively, NO production by nitrifier denitrification might continue for a short time at anoxia with oxidizing compounds stored in the form of NH_2OH or oxidized cytochromes.

NO decrease after NO_2^- addition. O_2 concentrations remained stable upon the addition of NO_2^-, which prevented switching between Aox and heterotrophic denitrification that could affect NO. Thus, the instantaneous decrease of NO after reaching the peak concentration (Figures 4a and b) might be regulated by direct effects on the enzymes involved in NO turnover within the bacteria that produce NO. This is supported by earlier studies, which showed that Nir and Nor can be inhibited by high NO concentrations in heterotrophic denitrifiers (Dhesi and Timkovich, 1984; Carr and Ferguson, 1990; Koutny and Kucera, 1999).

The model (Figure 1) suggests that the transient NO maximum after the addition of NO_2^- was due to an imbalance of the AOB metabolism (Sh, Equation (7)). Moreover, the decrease of the measured concentration from the maximum was slower than the modeled decrease by diffusion only (Figure 4a, black line and Figure 4c, filled triangles), indicating that NO production continued during the decrease. The model showed that if nitrifier denitrification is the only NO-producing process under oxic conditions, NO increased slowly after NO_2^- was added (Figure 4c, filled circles). Therefore, we propose that the direct formation of NO instead of NO_2^- continues with a decreasing rate after it becomes active. This implies that NO or NO_2^- concentrations directly affect the enzymes of AOB, resulting in the regulation of the metabolic imbalance.

Significance to NO and N_2O formation in the environment

The extent of transient NO and N_2O accumulation upon perturbation strongly indicates that it can significantly contribute to emissions of gaseous N oxides into the atmosphere, especially from habitats exposed to fluctuations in O_2 and inorganic N compounds. It is possible that the large uncertainties about the sources in the global N_2O budget (Stein and Yung, 2003) are linked to the contribution of fluctuating emissions from ecosystems, which are not normally considered during measurements (for example, measurements in chambers often impede exposure to environmental fluctuations).

Fluctuations in environmental conditions that affect O_2 and NO_2^- concentrations and thus lead to NO and N_2O production may occur in soils as a result of drying and wetting, or by a variable fertilizer input. Furthermore, estuaries are exposed to a fluctuating N input through precipitation and fertilizer runoff from land. Large oceanic volumes are influenced by mixing of water masses with different O_2 and NO_2^- concentrations. For example, massive accumulation of N_2O was observed in the upper layer of the Arabian Sea during severe upwelling-induced hypoxia on the western Indian shelf (Naqvi *et al.*, 2000). Under these conditions, the upper layer of the water body is especially exposed to O_2 fluctuations caused by O_2 input through wave action. Hence, the fact that oceans are still considered a relatively minor source of N_2O in the global budget might be an underestimate linked to difficulties in measuring and modeling N_2O emissions during frequently occurring, short-term environmental perturbations in marine waters. Presently, a linear, empirical-derived framework is employed in large-scale N_2O emission models (Jin and Gruber, 2003; Duce *et al.*, 2008). The characteristics of the metabolic model, such as thresholds, dynamic function and shift function, developed in this study to describe transient production mechanisms, may represent an important step toward more mechanism-based modeling.

Conclusions

In conclusion, characterization of microenvironmental conditions is required to determine the source of NO and N_2O production in complex, stratified environments. The presence of O_2 determines whether NO and N_2O are produced by AOB or by heterotrophic denitrifiers. Interestingly, NO and N_2O formation by AOB does not require micro-oxic conditions if NO_2^- is present in high concentrations (mM range). On the other hand, NO production, but not N_2O production, by heterotrophic denitrifiers is almost independent of NO_2^- concentrations. The high temporal resolution achieved by microsensors allowed the measurement of highly dynamic NO and N_2O formation following the change in O_2 and NO_2^- concentrations. Interpretation of the results with a metabolic model showed that Aox and heterotrophic denitrification need to be actively performed to respond to perturbations in O_2 and NO_2^- with instantaneous NO and N_2O production. The resulting transient accumulation is counteracted within minutes by regulating the NO turnover in the biofilm. This occurs either because a different pathway becomes active or because enzymes involved in the production process are affected directly. At steady

state, NO concentrations are regulated by kinetic control of the consumption processes. In a complex environment, massive formation of NO and N_2O may occur if a metabolically active N-cycling community is exposed to an external perturbation.

Acknowledgements

We thank Phyllis Lam, Angela Schramm and the technical assistants of the Microsensor Research Group of the Max-Planck-Institute for Marine Microbiology, Bremen, for their practical support; Olivera Kuijpers, Aaron Beck and Peter Stief for critically reading the article and the Max Planck Society for funding.

References

Andersen K, Kjaer T, Revsbech NP. (2001). An oxygen insensitive microsensor for nitrous oxide. *Sens Actuator B-Chem* **81**: 42–48.

Arp DJ, Stein LY. (2003). Metabolism of inorganic N compounds by ammonia-oxidizing bacteria. *Crit Rev Biochem Mol Biol* **38**: 471–495.

Beaumont HJE, Lens SI, Reijnders WNM, Westerhoff HV, van Spanning RJM. (2004a). Expression of nitrite reductase in *Nitrosomonas europaea* involves NsrR, a novel nitrite-sensitive transcription repressor. *Mol Microbiol* **54**: 148–158.

Beaumont HJE, van Schooten B, Lens SI, Westerhoff HV, van Spanning RJM. (2004b). *Nitrosomonas europaea* expresses a nitric oxide reductase during nitrification. *J Bacteriol* **186**: 4417–4421.

Bergaust L, Shapleigh J, Frostegard A, Bakken L. (2008). Transcription and activities of NOx reductases in *Agrobacterium tumefaciens*: the influence of nitrate, nitrite and oxygen availability. *Environ Microbiol* **10**: 3070–3081.

Betlach MR, Tiedje JM. (1981). Kinetic explanation for accumulation of nitrite, nitric-oxide, and nitrous-oxide during bacterial denitrification. *Appl Environ Microbiol* **42**: 1074–1084.

Bock E, Schmidt I, Stuven R, Zart D. (1995). Nitrogen loss caused by denitrifying nitrosomonas cells using ammonium or hydrogen as electron-donors and nitrite as electron-acceptor. *Arch Microbiol* **163**: 16–20.

Broecker WS, Peng TH. (1974). Gas-exchange rates between air and sea. *Tellus* **26**: 21–35.

Carr GJ, Ferguson SJ. (1990). Nitric-oxide formed by nitrite reductase of *Paracoccus denitrificans* is sufficiently stable to inhibit cytochrome-oxidase activity and is reduced by its reductase under aerobic conditions. *Biochim Biophys Acta* **1017**: 57–62.

Colliver BB, Stephenson T. (2000). Production of nitrogen oxide and dinitrogen oxide by autotrophic nitrifiers. *Biotechnol Adv* **18**: 219–232.

Conrad R. (1996). Soil microorganisms as controllers of atmospheric trace gases (H-2, CO, CH4, OCS, N2O, and NO). *Microbiol Rev* **60**: 609–640.

Crutzen PJ. (1979). Role of NO and NO2 in the chemistry of the troposphere and stratosphere. *Annu Rev Earth Planet Sci* **7**: 443–472.

de Beer D, Schramm A, Santegoeds CM, Kuhl M. (1997). A nitrite microsensor for profiling environmental biofilms. *Appl Environ Microbiol* **63**: 973–977.

de Beer D, van den Heuvel JC. (1988). Response of ammonium-selective microelectrodes based on the neutral carrier nonactin. *Talanta* **35**: 728–730.

Dhesi R, Timkovich R. (1984). Patterns of product inhibition for bacterial nitrite reductase. *Biochem Biophys Res Commun* **123**: 966–972.

Duce RA, LaRoche J, Altieri K, Arrigo KR, Baker AR, Capone DG *et al.* (2008). Impacts of atmospheric anthropogenic nitrogen on the open ocean. *Science* **320**: 893–897.

Freitag A, Rudert M, Bock E. (1987). Growth of nitrobacter by dissimilatoric nitrate reduction. *FEMS Microbiol Lett* **48**: 105–109.

Goretski J, Zafiriou OC, Hollocher TC. (1990). Steady-state nitric-oxide concentrations during denitrification. *J Biol Chem* **265**: 11535–11538.

Hooper AB. (1968). A nitrite-reducing enzyme from *Nitrosomonas europaea*—preliminary characterization with hydroxylamine as electron donor. *Biochim Biophys Acta* **162**: 49–65.

James SL. (1995). Role of nitric-oxide in parasitic infections. *Microbiol Rev* **59**: 533–547.

Jin X, Gruber N. (2003). Offsetting the radiative benefit of ocean iron fertilization by enhancing N2O emissions. *Geophys Res Lett* **30**: 4.

Kampschreur MJ, Picioreanu C, Tan N, Kleerebezem R, Jetten MSM, van Loosdrecht MCM. (2007). Unraveling the source of nitric oxide emission during nitrification. *Water Environ Res* **79**: 2499–2509.

Kampschreur MJ, Tan NCG, Kleerebezem R, Picioreanu C, Jetten MSM, Loosdrecht MCM. (2008). Effect of dynamic process conditions on nitrogen oxides emission from a nitrifying culture. *Environ Sci Technol* **42**: 429–435.

Kartal B, Kuypers MMM, Lavik G, Schalk J, den Camp H, Jetten MSM *et al.* (2007). Anammox bacteria disguised as denitrifiers: nitrate reduction to dinitrogen gas via nitrite and ammonium. *Environ Microbiol* **9**: 635–642.

Kester RA, deBoer W, Laanbroek HJ. (1997). Production of NO and N2O by pure cultures of nitrifying and denitrifying bacteria during changes in aeration. *Appl Environ Microbiol* **63**: 3872–3877.

Konneke M, Bernhard AE, de la Torre JR, Walker CB, Waterbury JB, Stahl DA. (2005). Isolation of an autotrophic ammonia-oxidizing marine archaeon. *Nature* **437**: 543–546.

Koutny M, Kucera I. (1999). Kinetic analysis of substrate inhibition in nitric oxide reductase of *Paracoccus denitrificans*. *Biochem Biophys Res Commun* **262**: 562–564.

Kucera I. (1992). Oscillations of nitric-oxide concentration in the perturbed denitrification pathway of *Paracoccus denitrificans*. *Biochem J* **286**: 111–116.

Kucera I, Kozak L, Dadak V. (1986). The inhibitory effect of nitrite on the oxidase activity of cells of *Paracoccus denitrificans*. *FEBS Lett* **205**: 333–336.

Li YH, Gregory S. (1974). Diffusion of ions in sea-water and in deep-sea sediments. *Geochim Cosmochim Acta* **38**: 703–714.

Lipschultz F, Zafiriou OC, Wofsy SC, McElroy MB, Valois FW, Watson SW. (1981). Production of NO and N2O by soil nitrifying bacteria. *Nature* **294**: 641–643.

Morley N, Baggs EM, Dorsch P, Bakken L. (2008). Production of NO, N2O and N-2 by extracted soil bacteria, regulation by NO2- and O-2 concentrations. *FEMS Microbiol Ecol* **65**: 102–112.

Naqvi SWA, Jayakumar DA, Narvekar PV, Naik H, Sarma V, D'Souza W *et al.* (2000). Increased marine production of N2O due to intensifying anoxia on the Indian continental shelf. *Nature* **408**: 346–349.

Poth M, Focht DD. (1985). N-15 kinetic-analysis of N2O production by *Nitrosomonas europaea*—an examination of nitrifier denitrification. *Appl Environ Microbiol* **49**: 1134–1141.

Revsbech NP. (1989). An oxygen microsensor with a guard cathode. *Limnol Oceanogr* **34**: 474–478.

Rodionov DA, Dubchak IL, Arkin AP, Alm EJ, Gelfand MS. (2005). Dissimilatory metabolism of nitrogen oxides in bacteria: comparative reconstruction of transcriptional networks. *PLoS Comput Biol* **1**: 415–431.

Schmidt I, Bock E, Jetten MSM. (2001). Ammonia oxidation by *Nitrosomonas eutropha* with NO2 as oxidant is not inhibited by acetylene. *Microbiology* **147**: 2247–2253.

Schmidt I, van Spanning RJM, Jetten MSM. (2004). Denitrification and ammonia oxidation by *Nitrosomonas europaea* wild-type, and NirK- and NorB-deficient mutants. *Microbiology* **150**: 4107–4114.

Schreiber F, Polerecky L, de Beer D. (2008). Nitric oxide microsensor for high spatial resolution measurements in biofilms and sediments. *Anal Chem* **80**: 1152–1158.

Shaw LJ, Nicol GW, Smith Z, Fear J, Prosser JI, Baggs EM. (2006). *Nitrosospira* spp. can produce nitrous oxide via a nitrifier denitrification pathway. *Environ Microbiol* **8**: 214–222.

Stein LY, Yung YL. (2003). Production, isotopic composition, and atmospheric fate of biologically produced nitrous oxide. *Annu Rev Earth Planet Sci* **31**: 329–356.

Strous M, vanGerven E, Kuenen JG, Jetten M. (1997). Effects of aerobic and microaerobic conditions on anaerobic ammonium-oxidizing (Anammox) sludge. *Appl Environ Microbiol* **63**: 2446–2448.

Zacharia IG, Deen WM. (2005). Diffusivity and solubility of nitric oxide in water and saline. *Ann Biomed Eng* **33**: 214–222.

Zumft WG. (1997). Cell biology and molecular basis of denitrification. *Microbiol Mol Biol Rev* **61**: 533–616.

Zumft WG. (2002). Nitric oxide signaling and NO dependent transcriptional control in bacterial denitrification by members of the FNR-CRP regulator family. *J Mol Microbiol Biotechnol* **4**: 277–286.

Zumft WG. (2005). Nitric oxide reductases of prokaryotes with emphasis on the respiratory, heme-copper oxidase type. *J Inorg Biochem* **99**: 194–215.

Supplementary Information accompanies the paper on The ISME Journal website (http://www.nature.com/ismej)